Raman study of H-centre aggregation in psi -irradiated RbI: evidence for I_3^- and I_2^0 di-interstitial defects

1992 J. Phys.: Condens. Matter 4 2701

(http://iopscience.iop.org/0953-8984/4/10/031)

J. Phys.: Condens. Matter 4 (1992) 2701–2719. Printed in the UK

Raman study of H-centre aggregation in γ-irradiated RbI: evidence for I_3^- and I_2^0 di-interstitial defects

A M T Allen and J D Comins

Department of Physics and Condensed Matter Physics Research Unit, University of the Witwatersrand, Johannesburg PO Wits 2050, South Africa

Received 9 October 1991

Abstract. A series of annealing experiments have been carried out on RbI after γ-irradiation at 195 and 295 K. Optical absorption and Raman scattering measurements enabled halogen–defect interactions and annealing kinetics to be monitored. The results identified the I_3^- di-interstitial as the predominant halogen defect for both temperatures of irradiation. This is contrary to the results from other alkali halides, KI and KBr, where for the higher temperature of irradiation the I_3^- di-interstitials are superceded by large molecular aggregates (I_2). No evidence for these large clusters in RbI emerged from the present work. For the 295 K irradiation, in addition to the I_3^- form of the di-interstitial, the I_2^0 neutral molecule form was also identified. This latter form of di-interstitial has been suggested by theoretical calculations but has not been detected previously by Raman scattering in any alkali halide. Its lower stability and smaller concentration than the I_3^- complex suggest that it is not the favoured form of di-interstitial halogen defect.

1. Introduction

The process of creation of anion Frenkel pairs in irradiated alkali halides is now relatively well understood in terms of the excitonic mechanism. As discussed by Itoh (1982), Williams *et al* (1984, 1986, 1987), Agulló-López and Townsend (1980) and Chen *et al* (1990) the theory accounts satisfactorily for the production of widely separated F and H centres, the relationship between the intrinsic luminescence and defect yield and the directional nature of sputtering patterns. By contrast, the series of secondary reactions in which the primary defects, in particular the H centres, become mobile and are trapped either intrinsically or extrinsically is understood only partially. This aspect is the main concern of the present work.

Electron spin resonance studies (Van Puymbroeck and Schoemaker 1981) have established in great detail the structure of the paramagnetic interstitial halogen defects. These include intrinsic H centres which are stable at sufficiently low temperatures; H centres trapped singly at impurities, for example the H_{Na} and H_D centres; and most recently H centres in the form of paramagnetic dimers trapped at divalent impurities. However, a considerable body of work has established that the dominant di-interstitial halogen species and higher order H centre aggregates are diamagnetic: thus other techniques must be used to determine their structures. Of these, optical absorption has provided the bulk of the experimental observations and, in a number of instances, has been successfully combined with other methods.

The formation of di-interstitial halogen molecular complexes as the first H centre

0953-8984/92/102701 + 19 $04.50

aggregation product has been studied by Itoh and Ikeya (1967) and Marat-Mendes and Comins (1975, 1977a,b). Trapped di-interstitial halogen defects at divalent impurities have been inferred from a combination of optical absorption, production and annealing kinetics, and ionic thermocurrent measurements. They are also shown to play a pivotal role in 'first stage' F centre production near ambient temperature (Comins and Carragher 1980, 1981).

The structure of the dominant di-interstitial halogen defect has been most controversial. Various authors have proposed either the neutral halogen molecule X_2^0 occupying two neighbouring interstitial sites, or the X_3^- molecular ion formed by the association of a lattice halide ion with two H centres. For example, computational static lattice defect calculations by Catlow *et al* (1980) tend to favour the X_2^0 configuration over X_3^- from energetic considerations. As a further possibility these authors also showed that the movement of anions and cations from their sites and the occupation of the resultant vacancy pairs by X_2^0 or X_3^- was energetically favourable; this exothermic reaction is postulated to lead to the perfect dislocation loops observed in the electron microscope (Hobbs *et al* 1973). The calculations again favoured the X_2^0 configuration to some degree. Studies of the V_4 centre in KBr by Mitsushima *et al* (1976) using ion beam channelling were also analysed in terms of the X_2^0 structure. On the other hand, the molecular orbital calculations of Okada and Hata (1981) accounted for the double peaks of the characteristic V band found near 3.6 eV and 4.4 eV in irradiated KI. In this case, the spin–orbit interaction in I_3^- ions in a variety of possible orientations is considered responsible for this structure. Similarly, Winter *et al* (1969) using a variety of alkali halides, concur with the earlier views of Hersh (1957), namely that the V band absorption arises from X_3^- ions. Most recently the combined use of Raman light scattering and optical absorption techniques has provided much new information concerning interstitial halogen aggregates (Lefrant and Rzepka 1979, 1980, Taurel *et al* 1983, Allen *et al* 1985, Allen and Comins 1987).

Raman studies of molecular halogen complexes have been carried out quite extensively. We shall concentrate on those relevant to the present study. The extent of interaction of the complex with its immediate environment results in a change in the Raman frequency shift. In certain cases, notably the I_3^- ion, such differences are rather small and the characteristic symmetric stretching vibration has a frequency $113 \pm 2\ cm^{-1}$ in water and methanol solutions (Maki and Forneris 1966, Klaboe 1967, Kiefer and Bernstein 1972, Kaya *et al* 1972), in matrix isolation studies (Andrews *et al* 1980) and in irradiated alkali halide crystals (Lefrant and Rzepka 1979, 1980, Allen *et al* 1985). Annealing experiments in which F and V optical absorption bands decayed simultaneously with the $113\ cm^{-1}$ Raman feature demonstrate that the di-interstitial I_3^- ion is a major complementary defect to the F centre in KI irradiated at 195 K (Allen *et al* 1985). Similar work on KBr attributed the V_4 optical absorption band to Br_3^- molecular ions (Rzepka *et al* 1987), a result contrary to the conclusions of Mitsushima *et al* (1976). Evidence for polyhalide ions such as I_n^- and Br_n^- has emerged from Raman studies (Loos and Jones 1974, Rzepka *et al* 1981, Taurel *et al* 1983). Formation of such clusters would be consistent with current ideas concerning the sequential trapping of H centres, beginning with the di-interstitial X_3^--type defect.

At higher irradiation temperatures there are significant changes in the nature of the halogen interstitial aggregates in many of the alkali halides; work in this regard has been carried out on KCl, KBr and KI using optical absorption and thermal conductivity measurements (Sonder and Walton 1967, Sonder and Sibley 1972). Increasingly large halogen interstitial clusters with higher temperature of irradiation have been postulated;

here Raman spectroscopy has provided significant new information. For example, the Raman spectrum in KI irradiated at 295 K exhibits two strong peaks at 180 and 189 cm^{-1}, the 113 cm^{-1} (I_3^-) and the 173 cm^{-1} (I_n^-) features being of negligible intensity (Lefrant and Rzepka 1980, Allen and Comins 1987). These transitions have been identified by comparison with Raman studies both in crystalline iodine and from matrix isolation work (Andrews *et al* 1980, Shanabrook and Lannin 1981). They are assigned to the I—I stretching mode of I_2 molecules in an aggregated form. Indeed, at sufficiently high dose, these large molecular clusters have been shown to take on a structured crystalline form; here low-frequency (<90 cm^{-1}) lattice modes of crystalline iodine have been observed (Taurel *et al* 1983).

Recently the intermediate regime has been studied by irradiation at temperatures between 195 and 295 K (Allen and Comins 1991). For such conditions all three halogen defect types: the I_3^- di-interstitial, the I_n^- polyhalide and the $(I_2)_n$ molecular clusters have been found to be present simultaneously. The $(I_2)_n$ clusters were already present after irradiation at 233 K and became dominant as the temperature of irradiation was increased. The progressive nature of the aggregation process from simple dimeric structures, such as I_3^-, to the large molecular complexes $(I_2)_n$ provides insights into the development of irradiation damage, particularly in the small-cluster regime, which in general has been difficult to study. The relationship between this cluster development and the large perfect dislocation loops has yet to be established. The suggested location of the I_3^- defects in vacancy triplets as considered by Catlow *et al* (1980) appears consistent with many of the experimental features; the aggregation of such defects (also considered theoretically by the same authors) could thus result in the observed higher order aggregates.

The apparent absence of the I_2^0 molecule as determined by Raman spectroscopy in irradiated KI we found somewhat intriguing, since it is theoretically predicted to be stable. There have been a number of Raman studies of the I_2 monomer. Using solution studies, Kiefer and Bernstein (1972) and Kaya *et al* (1972) showed that there is a range of frequencies for the I—I stretching mode of the I_2 molecule, from close to the gas phase value of 214 cm^{-1} in cases where the interaction with the solvent is weak, to values close to 200 cm^{-1} where stronger interaction occurs. There is also a characteristic optical absorption band; again the spectral position varies somewhat depending on the solvent. When the interaction with the solvent increases, the peak absorption moves towards higher energies (from approximately 2.5 to 2.7 eV). These authors also showed the effect of adding iodide salt to an iodine solution. In both cases the results were similar; the 2.7 eV absorption band and the 201 cm^{-1} Raman signal disappeared and were replaced by absorption bands at 3.3 and 4.4 eV and a Raman signal at 113 cm^{-1}. These are characteristic of the I_3^- ion.

In the present experiments on RbI we have examined the annealing behaviour of defects created by γ-irradiation at 195 and 295 K by a combination of Raman and optical absorption measurements. The results provide new information on the nature of the interstitial halogen complexes and identify important differences as compared with similar experiments on KI and KBr. In particular, evidence for the I_2^0 molecule created in RbI is presented; this is distinct from the I_3^- defects created simultaneously. A preliminary report on some of the work presented here has been published (Allen and Comins 1990).

2. Experimental technique

The nominally pure RbI single crystals used in this work were grown by the Laboratoire

de Physique Cristalline, Université de Nantes. For the room temperature irradiations a block of RbI was encapsulated in a pyrex envelope under a vacuum of 10^{-3} torr to avoid contamination. The irradiation was carried out at ambient temperature (approximately 295 K) for 250 h with γ-rays from a ^{60}Co source of strength 875 Ci. The crystal block was 3 cm from the source and the resulting irradiation dose was 250 Mrad. After irradiation, three suitable specimens of approximate size $10 \times 8 \times 1$ mm^3 were cleaved in turn from the crystal block, and mounted in a temperature-controlled optical cryostat. In the case of the 195 K irradiations, three similar sized samples of RbI to those described above were freshly cleaved, mounted in the optical cryostat and γ-irradiated with the same ^{60}Co source for 15 h. The samples were 10 cm from the source and the total dose was 1.5 Mrad.

Optical absorption measurements were carried out using a Cary 17 spectrophotometer. Raman studies used a Jarrell-Ash 1 m double-grating spectrometer fitted with an EMI 9863Q photomultiplier, and a PAR 1112 photon counting system. Raman spectra were excited with the 488 nm line of a Spectra-Physics 171 argon ion laser; the beam power at the sample was 50 mW, which was sufficiently low to avoid bleaching of the colour centres. All optical measurements were undertaken with the crystal temperature maintained at 80 K.

For the crystals irradiated at both 295 and 195 K, a series of annealing experiments were performed. For the 295 K irradiations, sample I(a) was isochronally annealed in steps of 10 K and optical absorption measurements were made between each anneal pulse. Sample I(b) was similarly isochronally annealed, but Raman scattering measurements were made between each anneal. In the isochronal anneals, care was taken to provide rapid heating and cooling for each pulse. Sample I(c) was subjected to a step anneal appropriate for a Primak activation energy analysis. This consisted of a series of isothermal anneals separated by 5 K intervals.

For the 195 K irradiations samples II(a) and II(b) were isochronally annealed, as described above for samples I(a) and I(b), and studied using optical absorption and Raman techniques, respectively. Sample II(c) was isothermally annealed and measured by optical absorption.

3. Analysis of annealing processes

In order to determine the reaction order and the characteristic activation energies of the annealing processes two different approaches were used: (a) that of Meechan and Brinkman (1956) and Garr and Sosin (1967a,b) and (b) the method of Primak (1955, 1956, 1960). The theoretical aspects will be described briefly here (complete treatments appear in the literature).

In methods (a), chemical rate theory is assumed, yielding the differential rate equation for an isothermal anneal as

$$\mathrm{d}n/\mathrm{d}t = -[\sigma^{\gamma-1} A \nu_0 \exp(-E/kT)]n^{\gamma} = -K(\gamma, E)n^{\gamma} \qquad (1)$$

Equation (1) refers to an anneal to completion in which the concentration of centres is n, initial concentration is n_0, the order of reaction is γ, the activation energy is E, the number of sites surrounding a centre at which the reaction can occur is σ and entropy and trap distribution factors are incorporated into A.

For the present case, in which a particular stage of annealing is considered and in which the optical absorption coefficient is experimentally determined, it follows that the incremental absorption coefficient $\Delta\alpha = \alpha - \alpha_\infty$ is the appropriate variable. Here α

represents the absorption coefficient related to the defect concentration by $\alpha = pn$ according to the Gaussian form of the Smakula equation (Dexter 1958) and α_∞ represents its value at the termination of the annealing stage.

Equation (1), recast in terms of $\Delta\alpha$ may be integrated to yield

$$\ln(\Delta\alpha_0/\Delta\alpha) = K(\gamma, E)t \qquad \text{for } \gamma = 1 \tag{2a}$$

$$(\Delta\alpha)^{1-\gamma} - (\Delta\alpha_0)^{1-\gamma} = K(\gamma, E)p^{1-\gamma}(\gamma - 1)t \qquad \text{for } \gamma > 1. \tag{2b}$$

These equations can be adapted to the case of an isochronal anneal in which Δt is the duration of an annealing step thus:

$$\ln(\Delta\alpha_{i-1}/\Delta\alpha_i) = K(\gamma, E)\,\Delta t \qquad \text{for } \gamma = 1 \tag{3a}$$

$$(\Delta\alpha_i)^{-1} - (\Delta\alpha_{i-1})^{-1} = K(\gamma, E)p^{-1}\,\Delta t \qquad \text{for } \gamma = 2. \tag{3b}$$

Equations (3*a*) and (3*b*)applied to the appropriate annealing routines permit γ and E to be calculated, using direct plots of the data on the assumption of a particular reaction order. Equation (2*b*) may also be written as

$$(\Delta\alpha)^{1-\gamma} = c(t + M). \tag{4}$$

Thus, with the correct choice of M, a plot of $\ln \Delta\alpha_i$ versus $\ln(t + M)$ should yield a straight line of slope $(1 - \gamma)^{-1}$. This permits the reaction order to be determined directly.

In method (b), the Primak approach permits an activation energy spectrum to be determined. It is of special usefulness in cases of complex annealing processes where a range of activation energies are involved. A brief account of the theory follows (the references contain detailed expositions).

For such a range of activation energies, the contribution to the optical absorption which anneals in the interval dE at E is $\alpha(E)\,dE$. The time rate of change of $\alpha(E)$ is

$$d\alpha(E)/dt = B\alpha(E)\exp(-E/kT) \tag{5}$$

where B is the effective frequency factor (assumed to be known approximately and to be the same for all the annealing processes). The solution to equation (5) is

$$\alpha(E) = \alpha_0(E)\exp[-Bt\exp(-E/kT)] = \alpha_0(E)\varphi(E,t,T). \tag{6}$$

Here $\alpha_0(E)$ is the original activation energy spectrum before any annealing has taken place, and $\varphi(E, t, T)$ represents the amount of the original distribution swept out as t increases. Assuming that $\alpha(E)$ can be approximated to a step function for small E intervals with average value $\bar{E}$ (and a corresponding absorption value $\alpha_{00}(\bar{E})$) it may be shown that these two parameters can be obtained from the following equations:

$$\bar{E} = \int_0^\infty EA_j\,dE \Big/ \int_0^\infty A_j\,dE \tag{7}$$

$$\alpha_{00}(\bar{E}) = (\alpha_{j-1}^{\text{total}} - \alpha_j^{\text{total}}) \Big/ \int_0^\infty A_j\,dE \tag{8}$$

where

$$A_j = \prod_{i=1}^{n-1} \varphi(E, t_i, T_i)[\varphi(E, t_{j-1}, T_n) - \varphi(E, t_j, T_n]\,dE. \tag{9}$$

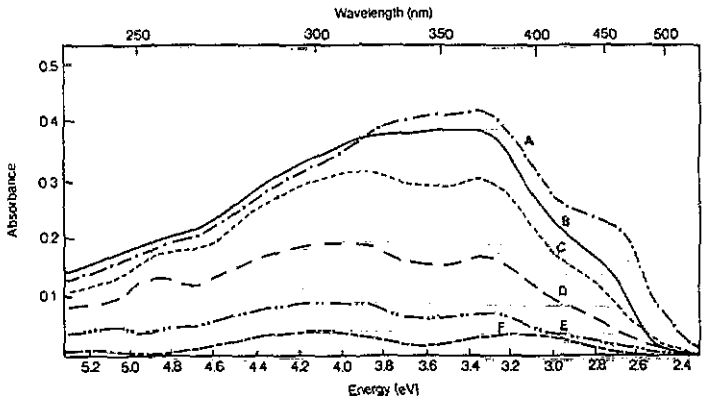

Figure 1. V band absorption spectra during the isochronal annealing of RbI after γ-irradiation at 295 K to a dose of 250 Mrad. Curves A to F correspond to annealing at temperatures of 318, 388, 418, 438, 448 and 453 K respectively. Spectra were measured at 80 K.

Here T_n is the temperature of the nth isotherm, t_{j-1} and t_j are successive anneal times on this isotherm, and T_i and t_i are the respective temperatures and total times of each of the forerunning isothermal anneals. With the aid of a computer program, the pairs of corresponding points $\alpha_{00}(\bar{E})$ and $\bar{E}$ were evaluated. The output is generated in the form of curve segments in which the most appropriate value of the frequency factor B provides the best fit for these segments. The activation energy spectrum thus generated requires extensive computation; the final output usually contains irregularities owing to the limited number of points, but nonetheless provides useful insights into the spectrum of activation energies.

4. Results

4.1. Room temperature irradiation (nominally 295 K)

The optical absorption spectrum of sample I(a) obtained after irradiation and prior to the isochronal anneal displayed a well-developed F band at 1.7 eV and a structured V band. The F centre concentration was determined as 1.9×10^{17} cm^{-3} using the Gaussian form of the Smakula equation and an oscillator strength assumed as 0.5.

The absorption in the V band is shown in figure 1. Trace A is equivalent to that obtained immediately after irradiation since no annealing had yet taken place. The accompanying set of spectra in figure 1 show the evolution of the V band envelope during the subsequent anneal. This leads initially to the disappearance of the 2.7 eV shoulder and to a change in spectral shape of the remaining absorption (traces B and C). The broad envelope resolved into a double-peaked structure, with peaks near 3.3 and 4.0 eV. Traces C to E of figure 1 show that these peaks decay together as the anneal is taken to completion.

The decay curves for the annealing of the F and V bands are shown in figure 2(a). The V band absorbance has been directly measured at 3.5 eV and thus represents an approximate overall behaviour for the complete envelope comprising several bands. The behaviour of the shoulder at 2.7 eV is also shown. The decay processes are seen to be quite complex. A broad overall picture identifies two main stages of annealing; stage

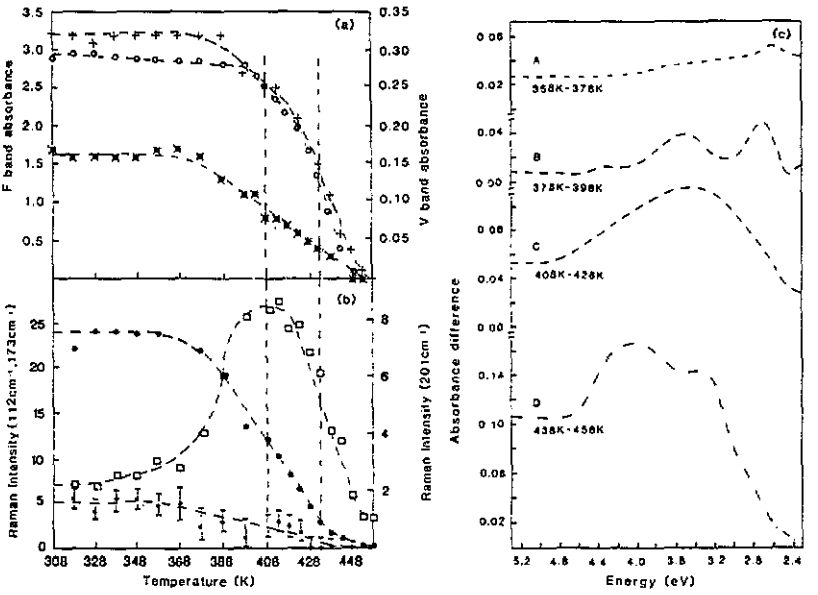

Figure 2. Decay curves for isochronal annealing experiments on two samples of RbI γ-irradiated at 295 K. (*a*) Annealing behaviour from optical absorption measurements: ○, F band; +, V band at 3.5 eV; ■, V band at 2.7 eV. (*b*) Annealing behaviour of defects from intensity of Raman bands: ●, 112 cm^{-1}; □, 173 cm^{-1}; *, 201 cm^{-1}. (*c*) Difference spectra in the ultraviolet. All measurements were made at 80 K.

I centred near 408 K and the higher temperature stage II, whose midpoint is near 433 K. Both stages have a width of approximately 40 K. In stage I the decay of the 2.7 eV feature occurs, with a partial reduction of the F band and the V band envelope. In stage II annealing, the reduction of the remaining and greater part of the F band and V band envelope occurs. These overlapping annealing processes are examined below, making use of the complementary Raman spectra and appropriate absorption difference spectra.

The Raman spectrum from sample I(b) obtained prior to annealing is presented in figure 3. The spectrum is dominated by the 112 cm^{-1} Raman band; in addition five overtones were resolved with the low laser power used. In order to examine the substructure between the fundamental and the first overtone, this spectral region has been magnified and is presented as an inset in figure 3. The Raman features include a broad band peaking at 173 cm^{-1} with a shoulder extending to approximately 140 cm^{-1}; they also include a feature not previously reported, at 201 cm^{-1}.

The changes in the Raman features at 201, 112 and 173 cm^{-1} during the anneal are shown in figure 2(*b*). The two broad stages of annealing present in the optical absorption are manifested in the behaviour of the Raman spectra. Stage I annealing centred at 408 K involves the decay of the 201 cm^{-1} feature, the reduction of the 112 cm^{-1} peak and its overtones and the accompanying growth of the 173 cm^{-1} band. Figure 4 shows this latter effect in detail: here the spectra are presented directly, including the first overtone at 224 cm^{-1}. Stage II annealing centred near 433 K is from the point of view of the Raman spectra concerned with the decay of the residual 112 cm^{-1} peak and of the 173 cm^{-1} band.

To assist in the correlation and interpretation of the somewhat complicated and overlapping processes involved in the annealing behaviour, a set of optical absorption

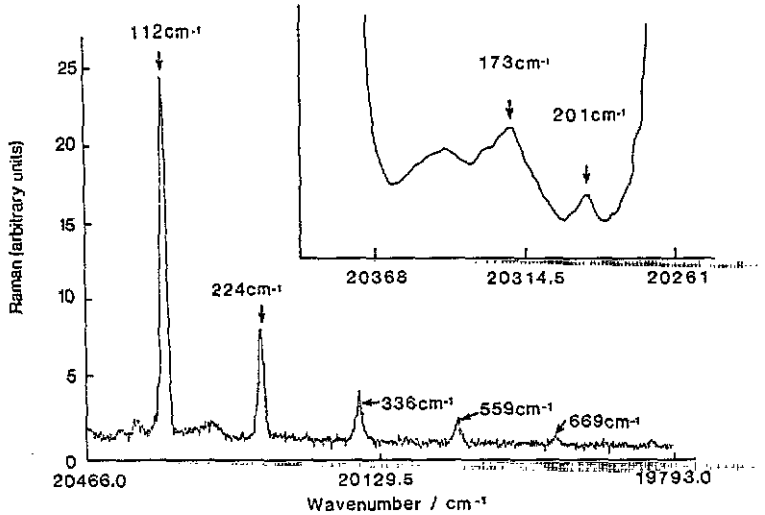

Figure 3. Raman spectrum obtained after γ-irradiation of RbI at 295 K to a dose of 250 Mrad. The main figure shows the 112 cm^{-1} band and its overtones. The inset is plotted on expanded scales (using a factor of ordinate expansion) and shows the structure between the 112 cm^{-1} fundamental and its first overtone. The spectrum was measured at 80 K. (λ_{laser} = 488 nm).

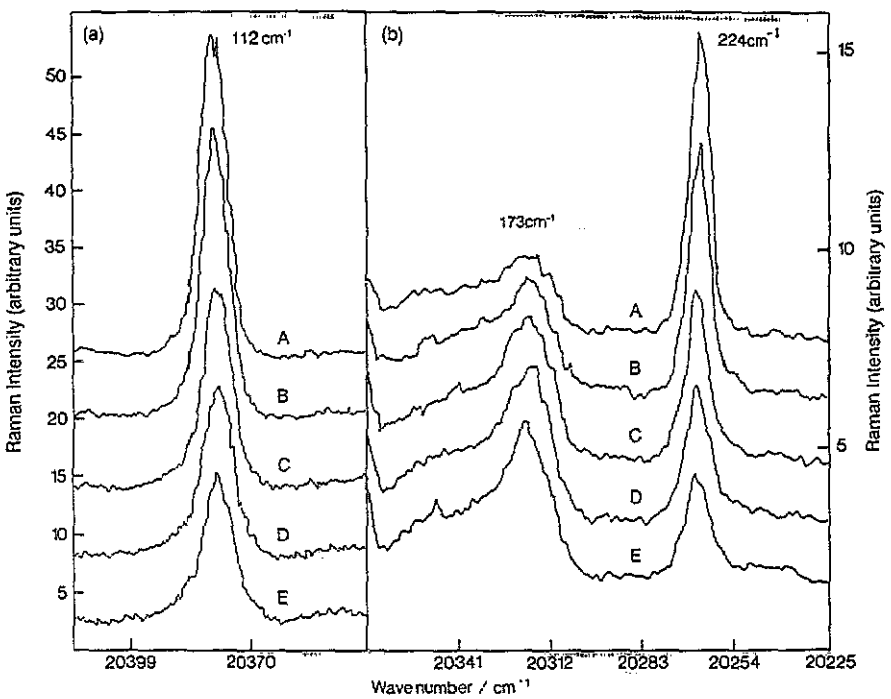

Figure 4. The concurring growth/decay of the 173 cm^{-1} band and the 112 cm^{-1} band. (*a*) The decay of the 112 cm^{-1} band. (*b*) The growth of the 173 cm^{-1} band and the concurrent decay of the 224 cm^{-1} band (first overtone of 112 cm^{-1}). Curves A to E are spectra obtained after annealing at 378, 388, 398, 408 and 413 K respectively.

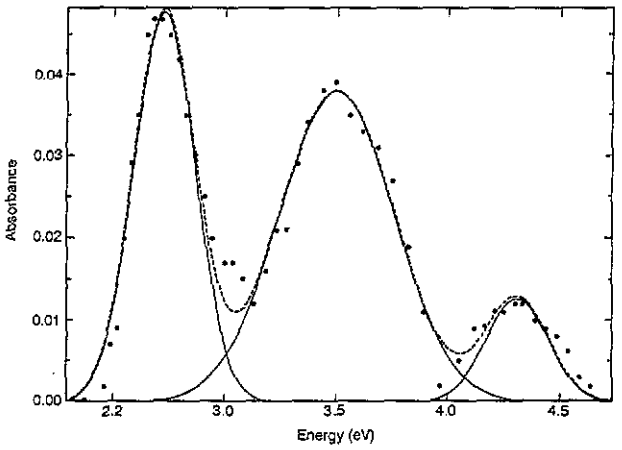

Figure 5. Deconvolution of the difference spectrum B shown in figure 2(*c*) indicating the presence of three components. Component band parameters: (energy in eV, width at half maximum in eV): (2.73, 0.32); (3.50, 0.62); (4.33, 0.35).

difference spectra corresponding to the spectral range 2.4 to 5.2 eV are presented in figure 2(c). In discussing these it is convenient to consider a number of temperature ranges in which the major changes occur. The following conclusions are drawn from an examination of the combined set of results.

(i) In the range 358 to 378 K (corresponding to difference spectrum A) it is seen from figure 2(*a*) that the first absorption features to decay are the bands at 2.7 and 3.5 eV beginning near 368 K. The total reduction is rather small. Within the precision of the measurements, the onset of decay appears essentially coincident. Examination of the F band indicates no appreciable change corresponding to the reduction in absorption of the 2.7 and 3.5 eV bands. The Raman spectra reveal some interesting correlations. The bands at 201 and 112 cm^{-1} begin to decay near 368 K in concert with the 2.7 and 3.5 eV absorptions respectively. These decreases are accompanied by an increase in 173 cm^{-1} Raman band.

(ii) In the range 378 to 398 K (difference spectrum B) more substantial decreases in the 2.7 and 3.5 eV bands occur. A weaker 4.3 eV band associated with the 3.5 eV band is also identified in this difference spectrum by its decay; in difference spectrum A its reduction is too small, to be recognized. The spectral shapes of these bands are clearly evident. A fit using three Gaussian bands employing a modified MINUIT deconvolution routine (James and Roos 1971) yielded the fit shown in figure 5, in which the band parameters are also given. Significantly, the shape of the V band envelope changes in this temperature region to the double-peaked structure mentioned earlier. This effect clearly results from the preferential reduction of absorption associated with the decay of the 3.5 eV band and its smaller associated band at 4.3 eV; it also establishes the presence of more stable V centres absorbing in the spectral region under examination. Within this temperature range, clear reductions in the F band and the overall V band envelope occur. The Raman bands at 201 and 112 cm^{-1} (together with the latter's overtones) continue to decay in this range; the 112 cm^{-1} decay is quite pronounced, as is the growth of the 173 cm^{-1} Raman feature.

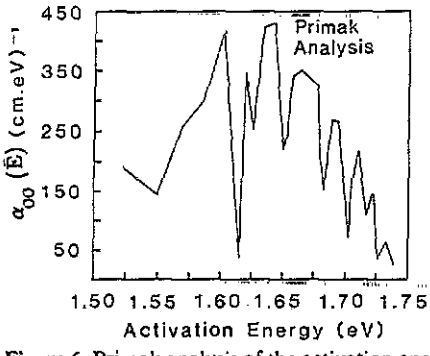

Figure 6. Primak analysis of the activation energy of annealing of RbI γ-irradiated at 295 K to a dose of 250 Mrad.

(iii) In the range 398 to 428 K, it is seen from difference spectrum C that decay in the V band envelope occurs over a broad spectral range from 2.4 to 4.8 eV. Examination of the V band envelopes shown in figure 1 shows that annealing of absorption bands peaking near 3.3 and 4.0 eV begins in this range; the broad decay thus reflects overlapping annealing processes incorporating further reduction of the 3.5, 4.3 and 2.7 eV bands, together with these 3.3 and 4.0 eV features. Corresponding to the onset of the 3.3, and 4.0 eV annealing there is an obvious increase in the rate of annealing of the F band near 418 K; we have now entered the regime of stage II annealing. The Raman spectra again show further reductions in the 201 and 112 cm^{-1} features; by now their intensities are quite low. The 173 cm^{-1} Raman band terminates its growth in this temperature range and begins to decrease.

(iv) In the latter part of the anneal, from 428 to 458 K, the dominant process is the annealing of the V bands peaking near 3.3 and 4.0 eV as shown in difference spectrum D and in the spectra of figure 1. Here it is evident that the F band and V band envelope are essentially annealing in parallel. The defects responsible for the 3.3 and 4.0 eV bands are a form of halogen interstitial. By this stage the Raman band at 112 cm^{-1} is very small and ultimately attains a zero value while the 201 cm^{-1} feature is negligible. The 173 cm^{-1} band completes its decay.

At this point it is convenient to examine the relationship of the 173 cm^{-1} Raman band to the measured optical absorption spectrum. As seen from the annealing data, there is significant growth in the 173 cm^{-1} band in the temperature range 368 to 408 K, followed by a decrease. In the region of most significant increase, 378 to 398 K there is no obvious increase in the optical absorption spectrum; indeed in the V band spectral region well-defined decreases occur in bands at 2.7, 3.5 and 4.3 eV. This aspect will be enlarged on in section 5.

Owing to the overall complexity of the annealing process, a Primak analysis was carried out using the data from the step anneal on sample I(c). The results are presented in figure 6 and indicate a range of activation energies between 1.50 and 1.75 eV with the most probable energies between 1.60 and 1.65 eV.

Since in stage I there are a number of overlapping processes without any single one being dominant, a direct study of the kinetics would not be expected to yield simple relationships. On the other hand in stage II, that is between about 418 and 448 K, the annealing is dominated by the mutual decay of F centres and the V centres absorbing at

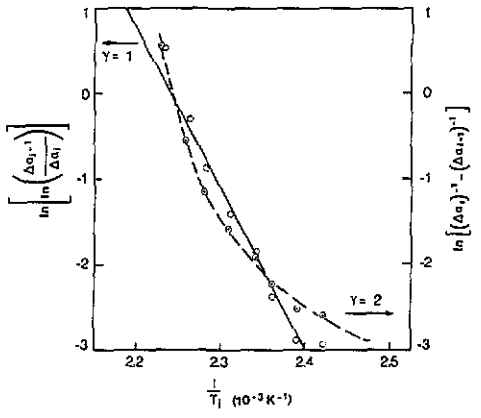

Figure 7. Plots to check reaction order and determine activation energy for stage II (412–448 K) of RbI annealing using the Arrhenius method. The results for $\gamma = 1$ give a reasonable fit and yield an activation energy of 1.6 eV; the plot for $\gamma = 2$ does not yield the required linear relation.

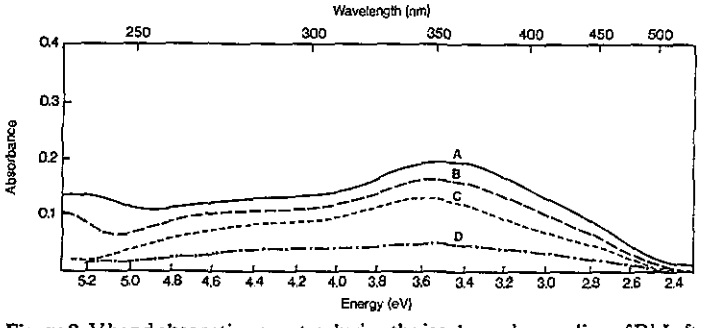

Figure 8. V band absorption spectra during the isochronal annealing of RbI after γ-irradiation at 195 K to a dose of 1.5 Mrad. Curves A to D correspond to annealing at 218, 268, 328 and 358 K respectively.

3.3 and 4.0 eV. Accordingly equation (3*a*) was used with the assumption of a reaction order of unity. The resulting plot for the F band appears in figure 7 and yields an activation energy of 1.6 ± 0.1 eV, in substantial agreement with the Primak results. Using equation (3*b*) for reaction order two gave a very non-linear behaviour also shown in figure 7. The reaction order of unity is significant and will be discussed further in the following section.

4.2. Irradiation at 195 K

The optical absorption spectrum produced after 1.5 Mrad γ-irradiation at 195 K included a prominent F band at 1.7 eV and a V band envelope with major peaks near 3.5 and 4.4 eV. The F centre concentration was $1.2 \times 10^{17}\,\mathrm{cm}^{-3}$, again assuming an oscillator strength of 0.5.

In figure 8 the optical absorption spectrum in the ultraviolet is shown at selected intervals during the isochronal anneal. Trace A is representative of that obtained

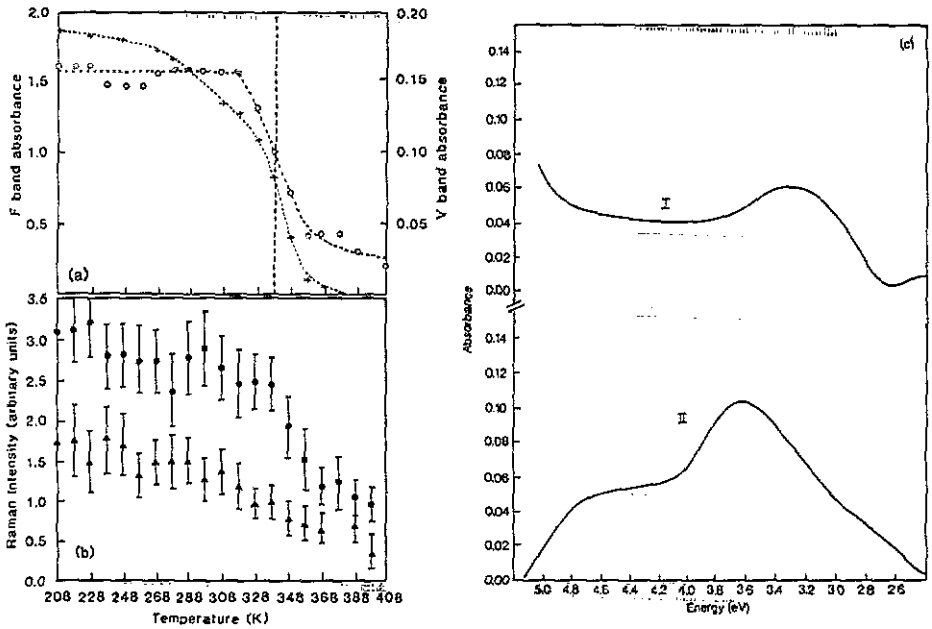

Figure 9. Decay curves for isochronal annealing experiments on two samples of RbI γ-irradiated at 195 K to a dose of 1.5 Mrad. (*a*) Annealing behaviour from optical absorption measurements: +, F band; ○, V band at 3.5 eV. (*b*) Annealing behaviour of defects from intensity of Raman bands: ●, 115 cm^{-1}; ▲, 163 cm^{-1}. (*c*) Difference spectra in the ultraviolet I, 208 K spectrum minus 308 K spectrum; II, 308 K spectrum minus 358 K spectrum.

immediately after irradiation, since no annealing had yet taken place. This spectrum, with its peaks near 3.5 and 4.4 eV is fairly similar to the bands close to these positions identified by difference spectrum B in figure 2(*c*). In the early stages of the anneal, the position of the larger peak moves slightly to approximately 3.6 eV, and thereafter the whole spectrum reduces together as the anneal is taken to completion.

The decay curves for the F band and the V band measured at 3.5 eV are shown in figure 9(*a*). The F band decay constitutes two stages: the first of these begins at about 260 K while the beginning of the second stage is near 320 K. The latter stage coincides with the decay of the V band envelope, represented by the 3.5 eV band.

The Raman spectrum of sample II(b) was unusually weak; the reason for this is not obvious. Nonetheless the spectrum was successfully extracted from contributions arising from weak laser plasma lines; here the final Raman spectrum after annealing was used for this purpose. The spectrum consists of a relatively sharp band near 115 cm^{-1} and a less intense broader band peaking at 163 cm^{-1}. Figure 10 displays a series of Raman spectra at various intervals during the isochronal anneal. It is seen that the 115 and 163 cm^{-1} bands decay. Curves C and D also indicate the presence of a weak contribution from the 173 cm^{-1} band partially underlying the 163 cm^{-1} feature. The decay of the Raman bands is plotted in figure 9(*b*). In spite of the relatively large measurement errors, complicated in the case of the 163 cm^{-1} band by the unresolved 173 cm^{-1} component, it can be seen that the two stages of F centre decay correlate reasonably well with the behaviour of the Raman bands. The decay of the 163 cm^{-1} band begins in the region of the first F centre annealing stage whereas the 115 cm^{-1} Raman band decays in the second stage.

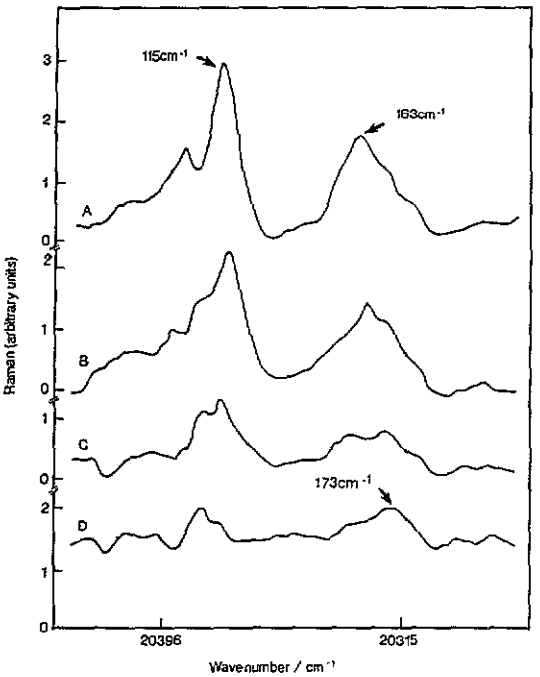

Figure 10. Raman spectra of RbI after γ-irradiation at 195 K to a dose of 1.5 Mrad. Spectra were measured at 80 K (λ_{laser} = 488 nm). A: after irradiation; B, C, D, after subsequent annealing at 268, 358 and 388 K respectively.

In order to examine further the annealing processes, appropriate difference spectra are plotted in figure 9(*c*) each lying within the respective annealing stages. Curve I was obtained by subtraction of the V band envelope produced after annealing at 308 K from the spectrum measured at 208 K; it shows that the major decay in stage I involves a V band peaking near 3.3 eV. It appears reasonable to associate this absorption with the 163 cm^{-1} Raman band. Curve II in the difference spectra (308 K spectrum minus 358 K spectrum) corresponds to the reduction in the V bands near the 3.6 and 4.4 eV spectral positions. This indicates that the latter absorptions are associated primarily with the 115 cm^{-1} Raman band, which decays together with the F band in stage II.

The main part of the V band annealing takes place in the second stage, centred near 343 K. The isochronal anneal figure 9(*a*) shows that the annealing of the 3.5 eV band is very steep; a choice of annealing temperature near the centre of this stage for an isothermal anneal would result in very rapid decay and provide insufficient data for a proper analysis. Accordingly the temperature for the isothermal anneal of sample II(c) was chosen as 308 K, close to the beginning of the second stage and near the end of the first stage. The remnant of the first stage would be rapidly exhausted over the time periods used, leaving the second stage to dominate. Two approaches were used to determine the order of the reaction: the Arrhenius method employing equations (2*a*) and (2*b*) for first- and second-order reactions respectively, and the Meechan and Brinkman method employing equation (4). The results are convincingly consistent and clearly indicate a second-order reaction as shown in figure 11.

On the basis of a second-order reaction, the activation energy for the process was found from the isochronal anneal using the Arrhenius method (equation (3*b*)). Figure

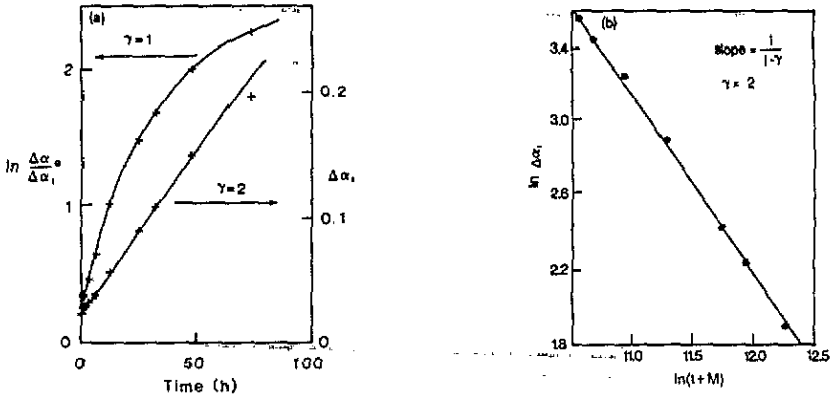

Figure 11. Determination of the order of reaction for F centre–interstitial recombination in the 338 K annealing step. (*a*) Using the Arrhenius method: results indicate a second-order ($\gamma = 2$) reaction. (*b*) Using the Meechan and Brinkman method.

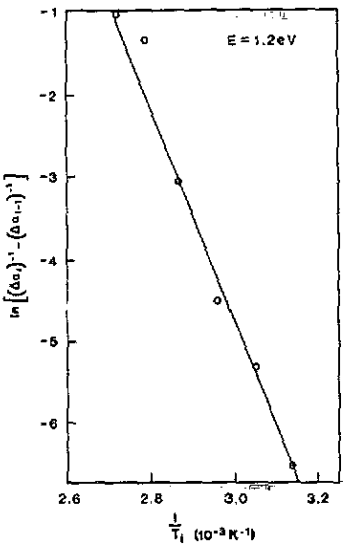

Figure 12. Determination of the activation energy E (1.2 eV) for the annealing process at 338 K using the Arrhenius method.

12 shows the fit obtained; the value of the energy determined from the slope of the graph is 1.2 eV.

5. Discussion

5.1. Irradiation at room temperature

The complex shape of the optical absorption spectrum obtained after irradiation and shown in figure 1 indicates a range of types of interstitial halogen defects. Nonetheless

the combination of techniques and comparisons with previous investigations discussed in the Introduction permit substantial progress to be made in their identification.

In contrast to the results on KI and KBr, where thus far only the X_3^- defect has been identified, the present work on RbI for irradiation at room temperature provides, for the first time, concurrent evidence for both postulated forms of dimeric halogen cluster; these are the I_3^- ion and the I_2^0 neutral molecule.

We consider first the I_3^- ion centres. It is clearly observed from the difference spectra A to C in figure 2(*c*) that a substantial part of the V band envelope results from absorptions peaking near 3.5 and 4.3 eV, the latter being a weaker component. As discussed in the Introduction these bands are characteristic of the I_3^- ion; slight variations in their peak positions have been noted previously (Okada and Hata 1981). Furthermore, the 112 cm^{-1} Raman band and its overtones match the decay of these absorption bands, as seen by observation of both difference spectra and the decay curves shown in figure 2. Reduction of the F band occurs during the decay of the 3.5 and 4.3 eV peaks of the absorption spectrum and with the decay of the 112 cm^{-1} Raman peak; comparison of the annealing curves shows that stage I of F centre decay is associated with these processes. Our results are also consistent with available thermoluminescence data. Sastry *et al* (1987) showed the presence of two thermoluminescence glow peaks in barium-doped RbI which was γ-irradiated at room temperature. The lower temperature peak at 370 K appears at both low and higher doses and is probably associated with interstitial halogen trapped in association with impurities; the higher temperature peak at 410 K found for high-dose irradiation accords well with our work on the first stage of F centre annealing.

The presence of a large number of overtones in the I_3^- Raman spectrum in RbI is accounted for by the near-resonance Raman excitation conditions (NRRE) employed. These are more nearly satisfied by RbI than KI for the 488 nm laser excitation used. This interpretation is supported by the observation of a weaker overtone series produced by Rzepka *et al* (1988) when further off-resonance, using the 514.5 nm laser line and a stronger series using the 457.9 nm line.

We now consider the I_2^0 neutral molecule centres. A further important effect during the broad stage I of the annealing is the simultaneous reduction of the 2.7 eV absorption band and the 201 cm^{-1} Raman band. As discussed in the Introduction, these are signatures of the I_2^0 neutral molecule; the vibrational frequency is lowered from the gas phase value, while the peak absorption energy is increased by interaction with the polar crystalline environment. The weak intensity of the 201 cm^{-1} Raman signal relative to that of the 112 cm^{-1} peak is in accord with the work done on iodine in solution by Kiefer and Bernstein (1972) and by Kaya *et al* (1972) and discussed in the Introduction.

It follows that the present studies have identified the simultaneous presence of I_3^- and I_2^0 in RbI irradiated near room temperature. The Raman and optical absorption features characteristic of these dimeric halogen aggregates are completely consistent with a variety of previous investigations on these species performed in the gas phase, in solution and by matrix isolation methods.

Subsequent to irradiation the Raman feature attributed to polyhalide I_n^--type defects is seen to exhibit a peak at 173 cm^{-1} superimposed on a broad underlying band. In their Raman work on the alkali iodides, Lefrant and Rzepka (1980) found a similar, though weaker Raman spectrum for RbI after x-irradiation at 293 K; their band near 170 cm^{-1} exhibited a slightly different shape. A later experiment by Rzepka *et al* (1981) resulted in a Raman spectrum rather similar to that of figure 3 despite a γ-ray dose four times that of our experiments.

The 173 cm^{-1} band in RbI, like its counterpart in KI, is associated with I_n^- polyiodide defects (Andrews 1972, Loos and Jones 1974). The breadth of the band and its changing appearance with irradiation conditions suggests a range of I_n^- defects, each with its own characteristic vibrational signal. Raman studies of halide ions in solution and in a solid matrix as discussed in the Introduction, have suggested frequencies in the range 140 to 173 cm^{-1} for higher order polyiodides.

It is noteworthy that the initial consequence of the reduction in concentration of both I_3^- and I_2^0 is the rise in the magnitude of the 173 cm^{-1} Raman band. This begins at about 360 K, which is significantly lower than the obvious annealing of the F band in stage I. On this basis the growth of this feature would be satisfactorily accounted for by the reaction $I_3^- + I_2^0 \rightarrow I_5^-$. Higher order aggregates could be formed similarly. It seems significant that in annealing experiments conducted on KI in which I_3^- defects were present, but I_2^0 was not evident, there occurred no obvious growth of the 173 cm^{-1} feature (Allen *et al* 1985). Since there is also a small reduction in the F band during the process of interconversion to I_n^- defects, it is apparent that a fraction of the dimeric clusters recombine with F centres.

Returning to the decay curves in figure 2(*a*) and (*b*) one might expect to associate a component of the V band envelope with the I_n^- defects. However, as already mentioned, careful examination of the difference spectra in figure 2(*c*) does not suggest a significant growth of absorption which could be attributed to these defects. It thus appears that the I_n^- defects have weak absorption which could also be spectrally broad; they could also be in low concentration. Near-resonance Raman scattering could well be responsible for the fairly strong Raman signals for these defects.

As observed from the V band envelope decay curves and from the difference spectra, the dominant annealing process between 428 and 458 K involves the mutual decay of the F band together with V bands peaking near 3.3 and 4.0 eV. Although the 173 cm^{-1} Raman feature associated with the I_n^- aggregates also decays in this stage of the anneal, it is not thought that the 3.3 and 4.0 eV absorptions are associated with them. As discussed above, no obvious growth of absorption in these spectral positions occurred during the growth phase of the 173 cm^{-1} Raman band.

We therefore suggest that, in view of the first-order kinetics found for the F–V annealing process in this temperature range, the responsible defects are a form of large halogen interstitial cluster which is Raman inactive. The defects are not in the form of the large iodine molecular aggregates $(I_2)_n$ found in KI, owing to the absence of the characteristic and strong Raman doublet at 180 and 189 cm^{-1}. Their contribution to the total halogen defect inventory is substantial, corresponding to approximately 30% of the F centre concentration with which they anneal.

5.2. Irradiation at 195 K

The absorption spectrum obtained at 195 K is considerably less complex than that obtained at room temperature. Indeed, the annealing processes and difference spectra attest to this and suggest that a limited variety of defects are present. The dominant peaks at 3.5 and 4.4 eV are characteristic of the I_3^- molecular ion as previously discussed. Similarly, the occurrence of the 115 cm^{-1} Raman transition confirms their presence (small wavenumber shifts of ± 2 cm^{-1} have been observed in studies of these complexes; their origin is presumably associated with slightly differing environments).

The main annealing stage centred near 343 K involving reduction in absorption near 3.5 and 4.4 eV with the simultaneous decay of the F band and the 115 cm^{-1} Raman band

is characterized by second-order kinetics. The results are consistent with a process in which well-dispersed dihalogen complexes (I_3^- centres) annihilate with their complementary F centres. The activation energy of 1.2 eV is quite close to the value of 1.4 eV obtained in KI, similarly irradiated and annealed and involving I_3^- centres; here too second-order kinetics were observed (Allen *et al* 1985).

The larger halogen clusters created by room temperature irradiation of RbI are clearly absent in this case. It is also interesting to note that there is no trace of the optical absorption at 2.7 eV characteristic of I_2^0 for this 195 K irradiation; nor is there an observable Raman band at 201 cm^{-1}. Thus the I_2^0 neutral molecule is not the favoured form of di-interstitial even for low-temperature irradiation.

The Raman peak at 163 cm^{-1} will now be examined. An inspection of the annealing curves presented in figure 9(*a*) and (*b*) shows that the 163 cm^{-1} band reduces during stage I of the F centre annealing. Furthermore, the difference spectra of figure 9(*c*) indicate the reduction of a V band peaking near 3.3 eV in the same temperature region. We suggest that the 163 cm^{-1} Raman band and the 3.3 eV optical absorption band are due to the same defect and that this is some form of halogen interstitial. It should be noted that Lefrant and Rzepka (1980) observed a similar Raman band at 160 cm^{-1} on irradiating RbI at 100 K; they observed that as the irradiation temperature was increased this feature decreased in intensity.

The 163 cm^{-1} Raman band is distinct from the 173 cm^{-1} band due to the I_n^- complexes. We noted the small intensity of the 173 cm^{-1} band as an underlying component. For the 173 cm^{-1} band, an associated absorption was not obvious (section 4.1). Furthermore from a comparison of the relative magnitude of the annealing processes presented in figure 9, it is seen that the later stage involving the I_3^- molecular halogen complexes dominates; the halogen interstitials responsible for the 163 and 173 cm^{-1} Raman features are of relatively minor importance for an irradiation at 195 K.

6. Summary and conclusions

A combination of Raman and optical absorption spectroscopy in conjunction with annealing techniques has identified several types of halogen interstitial complexes in irradiated RbI. This work has clarified the controversy regarding the structure of the dominant dimeric interstitial cluster in the compound. The I_3^- halogen complex accounts for a substantial fraction of the H centres formed in the primary defect formation process during irradiation at both 195 and 295 K. The analysis of annealing results for the reduction of I_3^- defects created at 195 K indicates an activation energy of 1.2 eV, and a second-order reaction implying widely separated di-interstitial complexes. In the case of the 295 K irradiation, some interstitial halogen is in the form of I_2^0 neutral molecules. These defects are identified definitively for the first time and exist simultaneously with the apparently more numerous I_3^- complexes. Partial conversion of I_2^0 and I_3^- to higher order clusters I_n^- takes place; these latter defects have at most weak optical absorption. For 295 K irradiation, a significant fraction of the halogen interstitials exist in the form of larger Raman-inactive halogen clusters which anneal near 433 K with first-order kinetics and an activation energy with a most probable value near 1.6 eV. In the case of the 195 K irradiation a relatively small contribution to the halogen interstitial inventory arises from interstitial halogen defects absorbing near 3.3 eV and having a Raman transition near 163 cm^{-1}.

A comparison of RbI and KI irradiated at 195 K shows that the I_3^- complex anneals at the same temperature, 338 K. In the former case the activation energy was 1.2 eV, in the latter 1.4 eV. On the other hand, for 295 K irradiation the I_3^- complexes were produced in significant concentration in RbI, whereas they were negligible in KI. It should be pointed out that the structure of the I_3^- defects formed at 295 K in RbI must be different from those produced at 195 K, since they begin to anneal near 360 K, a significantly higher temperature. Structurally different I_3^- complexes have been considered by Catlow *et al* (1980) and Okada (1981).

The formation of larger clusters of interstitial halogen which have a crystalline iodine form at very high doses in KI has been established (Taurel *et al* 1983). The aggregation process in RbI appears to be different. Although a form of large interstitial cluster is apparent, its structure is not the same as the KI case. Indeed the significant presence of I_3^- for 295 K irradiations of RbI suggests that the factors controlling the efficient formation of the large $(I_2)_n$ clusters in KI are absent in RbI. The migration of I_3^- defects, either intrinsic or bound to trivacancies (Catlow *et al* 1980) needs to be investigated fully before these aggregation processes can be understood. Further theoretical calculations of the structure and mobility of the defect complexes particularly in RbI, would be very valuable.

Acknowledgments

We thank Professor S Lefrant and Dr E Rzepka of the Laboratoire de Physique Cristalline, Institute de Physique et Chimie des Matériaux, Université de Nantes, France for providing the sample of RbI. We are grateful to Professor R J Keddy and Dr T Nam of the Schonland Research Centre for Nuclear Sciences, University of the Witwatersrand for making the ^{60}Co γ-ray facility available to us. We thank the Foundation for Research Development for funding our research activity.

References

Agulló-López F and Townsend P D 1980 *Phys. Status Solidi* b **97** 575
Allen A M T and Comins J D 1987 *Cryst. Latt. Defects Amorph Mater.* **17** 93
—— 1990 *Nucl. Instrum. Methods* B**46** 240.
—— 1991 *Nucl. Instrum. Methods* B at press
Allen A M T, Comins J D and Ford P J 1985 *J. Phys. C: Solid State Phys.* **18** 5783
Andrews L 1972 *J. Chem. Phys.* **57** 51
Andrews L, Prochaska E S and Loewenschuss A 1980 *Inorg. Chem.* **19** 463
Catlow C R A, Diller K M and Hobbs L W 1980 *Phil. Mag.* A**42** 123
Chen L F, Song K S and Leung C H 1990 *Nucl. Instrum. Methods* B**46** 207
Comins J D and Carragher B O 1980 *J. Physique Coll.* **41** C6–166
—— 1981 *Phys. Rev.* B**24** 283
Dexter D L 1958 *Solid State Physics* ed F Seitz and D Turnbull (New York: Academic)
Garr K R and Sosin A 1967a *Phys. Rev.* **162** 669
—— 1967b *Phys. Rev* **162** 681
Hersh H N 1957 *Phys. Rev.* **105** 1410
Hobbs L W, Hughes A E and Pooley D 1973 *Proc. R. Soc.* A**332** 167
Itoh N 1982 *Adv. Phys.* **31** 491
Itoh N and Ikeya M 1967 *J. Phys. Soc. Japan* **22** 1170
James F and Roos M 1975 *Comput. Phys. Commun.* **10** 343
Kaya K, Mikami N, Udagawa Y and Ito M 1972 *Chem. Phys. Lett.* **16** 151

Kiefer W and Bernstein H J 1972 *Chem. Phys. Lett.* **16** 5
Klaboe P 1967 *J. Am. Chem. Soc.* **89** 3667
Lefrant S and Rzepka E 1979 *J. Phys. C: Solid State Phys.* **12** L573
Lefrant S and Rzepka E 1980 *J. Physique Coll.* **41** C6–476
Loos K R and Jones A C 1974 *J. Phys. Chem.* **78** 2306
Maki A G and Forneris R 1966 *Spectrochim. Acta* A**23** 867
Marat-Mendes J N and Comins J D 1975 *Cryst. Latt. Defects Amorph. Mater.* **6** 141
—— 1977a *J. Phys. Chem. Solids* **38** 1003
—— 1977b *J. Phys C: Solid State Phys.* **10** 4425
Meechan C J and Brinkman J A 1956 *Phys. Rev.* **103** 1193
Mitsushima Y, Morita K, Matsunami N and Itoh N 1976 *J. Physique Coll.* **37** C7–95
Okada T and Hata J 1981 *Mol. Phys.* **43** 1151
Okada T 1981 *J. Phys. Soc. Japan* **50** 582
Primak W 1955 *Phys. Rev.* **100** 1677
—— 1956 *Phys. Rev.* **103** 1681
—— 1960 *J. Chem. Phys.* **22** 1689
Rzepka E, Lefrant S, Taurel L and Hughes A E 1981 *J. Phys. C: Solid State Phys.* **4** L767
Rzepka E, Bernard M and Lefrant S 1988 *Nucl. Instrum. Methods* B**32** 235
Rzepka E, Bernard M, Lefrant S and Comins J D 1987 *Cryst. Latt. Defects Amorph. Mater.* **17** 113
Sastry S B S, Muralidharan G and Nagarajan S 1987 *Cryst. Latt. Defects Amorph. Mater.* **17** 211
Shanabrook B V and Lannin J S 1981 *Solid State Commun.* **38** 49
Sonder E and Walton D 1967 *Phys. Lett.* A**25** 222
Sonder E and Sibley W A 1972 *Point Defects in Solids* vol 1, ed J H Crawford and L M Slifkin (New York: Plenum)
Taurel L, Rzepka E and Lefrant S 1983 *Radiat. Eff.* **72** 115
Van Puymbroeck W and Schoemaker D 1981 *Phys. Rev.* B**23** 1670
Williams R T, Craig B B and Faust W L 1984 *Phys. Rev.* B**33** 1709
Williams R T and Song K S 1987 *Cryst. Latt. Defects Amorph. Mater.* **17** 151
Williams R T, Song K S, Faust W L and Leung C H 1986 *Phys. Rev.* B**33** 7232
Winter E M, Wolfe D R and Christy R W 1969 *Phys. Rev.* **186** 949